A Quantitative Comparison of Electrode Positions for Respiratory Surface EMG

Andra Oltmann, Jan Graßhoff, Nils Lange, Tobias Knopp and Philipp Rostalski

***Abstract*— Objective: Respiratory surface electromyography (sEMG) is a promising physiological signal for analyzing respiratory effort, patient-ventilator asynchrony, and respiratory training. In clinical research, a wide variety of different setups are used and no consensus has yet been reached on the positioning of electrodes. Therefore, this work aims to quantitatively compare both unilateral and bilateral bipolar electrode leads. Methods: Recordings of diaphragmatic and intercostal muscle activity were performed in 20 young and healthy adults using a setup with 64 electrodes placed in relation to prominent anatomical lines. Subjects completed three breathing maneuvers: 300 s quiet breathing, 5 maximum inspiratory pressure (MIP) trials, and 15 breaths of resistance breathing at 20 % of the MIP. To quantify the performance of differential electrode leads, three metrics were determined: the ratio between inspiratory muscle activity and (1) baseline noise (SNR_{base}), (2) expiratory muscle activity (SNR_{exp}), and (3) ECG interference ($SNR_{EMG-ECG}$). Results: The study revealed considerable differences between bipolar electrode positions. Our results support the use of bilateral positions on the midclavicular line and parasternal line for measuring diaphragm and intercostal activity. For intercostal muscles, there is a high flexibility in positioning electrodes more lateral or medial, if necessary. Unilateral leads do not appear to outperform the bilateral configuration as SNR metrics were consistently smaller. Conclusion: This study provides recommendations for electrode placements and is a first step towards standardization of respiratory sEMG measurements. Significance: This electrode lead standardization will be essential to increase clinical acceptance in the future.**

***Index Terms*— electrode positioning; respiratory muscles; surface electromyography;**

This work was funded by European Union - European Regional Development Fund, the Federal Government and Land Schleswig-Holstein, Project: "Diagnose- und Therapieverfahren für die Individualisierte Medizintechnik (IMTE)", Project No.: 12 420 002. Jan Graßhoff and Philipp Rostalski hold multiple patents with Drägerwerk AG & Co. KGaA and have received research grants and speaking fees from Drägerwerk AG & Co. KGaA. (*Corresponding author: Andra Oltmann.)*

Andra Oltmann, Jan Graßhoff, Nils Lange, Tobias Knopp and Philipp Rostalski are with the Fraunhofer IMTE, Fraunhofer Research Institution for Individualized and Cell-Based Medical Engineering, 23562 Lübeck, Germany (e-mail: andra.oltmann@imte.fraunhofer.de).

Tobias Knopp is also with the Institute for Biomedical Imaging, Hamburg University of Technology, Hamburg, Germany and with the Section for Biomedical Imaging, University Medical Center Hamburg-Eppendorf, Hamburg, Germany.

Philipp Rostalski is also with the Institute for Electrical Engineering in Medicine, University of Lübeck, Lübeck, Germany.

I. Introduction

RESPIRATORY electromyography (EMG) is a diagnostic method for recording the electrical muscle activity generated during spontaneous breathing. It has been used to analyze respiratory effort, patient-ventilator asynchrony, and respiratory muscle training in both intensive care and home mechanical ventilation [1]–[3].

Surface electromyography (sEMG) is an emerging method in which respiratory activity is measured completely non-invasively using standard gel electrodes located on the torso [3]. It is easy to use in clinical practice and also enables measurement of relevant respiratory muscles beyond the diaphragm, such as the intercostal muscles. However, due to the anatomy of respiratory muscles, their sEMG signals often have a relatively low signal-to-noise ratio and are strongly affected by crosstalk from other muscles. The most prominent contaminant is the electrocardiographic (ECG) artifact. Another important source of interference is the crosstalk between inspiratory and expiratory muscles in particularly when they are in close proximity as is the case with the internal and external intercostal muscles or with the diaphragm and abdominal wall muscles.

Research and clinical application of respiratory sEMG is currently hindered by the lack of standardisation of measurement setups and signal analyses [3]. Currently, there is no consensus yet on the electrode positioning and different studies have used widely different setups. As a consequence, the comparability of studies is limited, an estimation of performance reduction due to incorrect positioning is not possible, and the derivation of a clinical standard is difficult. An overview of previously used configurations is given in Table I.

For measuring the diaphragm's muscle activity, both bilateral and unilateral bipolar recordings have been proposed. In the most commonly used bilateral configuration, electrodes are placed on both sides of the rib cage at the intersection between the costal margin and the midclavicular line (MCL) or the nipple line [1], [2], [4]–[7]. Numerous other studies have placed electrodes in the 7th and 8th intercostal space, midway between the anterior (AAL) and mid-axillary lines (MAL), on one side of the torso [8]–[11]. Moreover, completely different unilateral setups have been employed to measure the diaphragm's compound muscle action potential (CMAP) during phrenic nerve stimulation [13], [14]. Here, a commonly used lead consists of one electrode positioned on the xiphoid process (XP) and a second electrode inferior to the first one on the costal margin.

TABLE I
OVERVIEW OF BIPOLAR LEADS USED IN RESEARCH AND CLINICAL APPLICATION OF RESPIRATORY SEMG

Electrode lead	Studies
Diaphragm	
●	Graßhoff *et al.* [1]; Sauer *et al.* [2]; Duiverman *et al.* [4]; Bellani *et al.* [5]; Duiverman *et al.* [6]; Pozzi *et al.* [7]
●	Estrada-Petrocelli *et al.* [8] (NSS); Lozano-Garcia *et al.* [9] (NSS); Ortega *et al.* [10] (NSS); Ràfols-de-Urquía [11] (RS)
●	Alonso *et al.* [12] (RS)
●	Younis *et al.* [13] (SS)
●	Younis *et al.* [13] (SS); Chen *et al.* [14] (SS)
Intercostal Muscles	
●	Graßhoff *et al.* [1]; Sauer *et al.* [2]; Bellani *et al.* [5]; Duiverman *et al.* [4]; Pozzi *et al.* [7]
●	Bureau *et al.* [15]; Schmidt *et al.* [16]
●	Ritz *et al.* [17] (RS)

Unilateral leads are drawn on the right side of the chest even if no specific body side has been specified or the lead has been used on either side of the body.
MAL: midaxillary line; AAL: anterior axillary line; MCL: midclavicular line; PSL: parasternal line; RS: right side; SS: stimulation side; NSS: no specific side or both sides

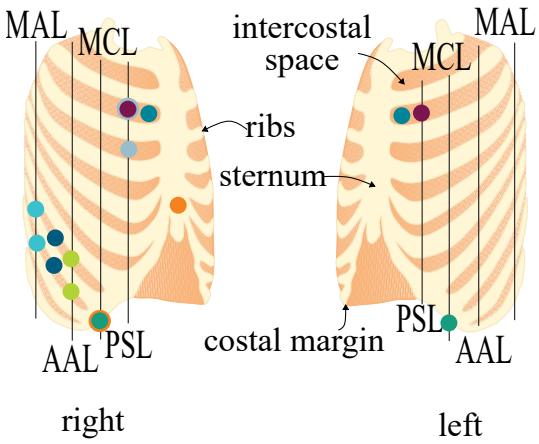

Most sEMG setups for measuring intercostal muscle activity have relied on bilateral leads. The setup with electrodes in the 2nd intercostal space on the parasternal line (PSL) or 2-3 cm from the margin of the sternum is the most commonly studied [1], [2], [4]–[7]. An alternative approach is to position electrodes bilaterally and directly adjacent to the sternum margin [15], [16]. Finally, a unilateral lead was applied in [17] using electrodes in the 2nd and 3rd intercostal spaces on the right side of the chest.

There is only a very limited number of studies that have compared different electrode setups for measuring respiratory activity, refer to [6], [18]–[20]. In [6] selected bipolar leads were analyzed for healthy subjects and COPD patients with regard to their reproducibility and their responsiveness to changes in respiratory load. Van Leuteren *et al.* [18] compared the bipolar arrangement at the intersection of the MCL and the costal margin with medially, laterally, inferiorly, or superiorly shifted setups in preterm infants. Additionally, in [19] the inspiratory sEMG activity in unilateral recordings with electrodes placed in intercostal spaces on various anatomical lines was investigated. However, to date, there is no comprehensive study that systematically investigates unilateral and bilateral electrode configurations for both intercostal muscle and diaphragm activity concerning performance metrics that address challenges of sEMG such as crosstalk and ECG interference.

In this study we develop a systematic and reproducible electrode scheme for recording the spatial distribution of electrical potentials generated on the skin surface, which enables us to conduct a quantitative comparison of electrode leads.

A preliminary version of this work has been reported [21].

II. METHODS

A. Study Population

The study included a cohort of 20 healthy adult subjects (10 males and 10 females). To be able to cover the general ICU population and to avoid particularly challenging signal acquisitions, the exclusion criterion for body-mass-index (BMI) was set at $50\,\mathrm{kg/m^2}$. The protocol was approved by the local ethics committee (University of Lübeck, Lübeck, Germany, reference no. 2023-480_1, June 2023) and all subjects declared written informed consent before participating.

B. Measurements

1) Electrode Positions: A total of 64 adhesive gel electrodes ($30 \times 24\,\mathrm{mm}$, Kendall H124SG, CardinalHealth, Dublin, Ireland) was placed according to the electrode scheme depicted in Fig. 1. Electrodes were positioned in relation to prominent anatomical lines, including the midaxillary line (MAL), anterior axillary line (AAL), midclavicular line (MCL), and parasternal line (PSL), as well as bony landmarks. The electrode scheme was developed to cover the diaphragm zone of apposition and the intercostal muscles, while also incorporating positions used in earlier studies. For electrodes positioned in the lower rib cage area, the intersection between anatomical lines and the costal margin was used as a reference, similar to [1], [2], [4]–[7]. From this bony landmark, arrays of electrodes were spaced with a vertical distance of $\mathrm{IED} = 25\,\mathrm{mm}$. Additionally, three electrodes were located in the 6th, 7th, and 8th intercostal space in between the MAL and AAL, labeled as inter axillary line (IAL), which coincides with [8]–[11]. One electrode was positioned $5\,\mathrm{cm}$ superior to the xiphoid process (XP), which is a location commonly used for measuring the diaphragm's compound muscle action potential [13], [14]. For placement in the upper rib cage region, the intersection between PSL and MCL with the 2nd and 3rd intercostal spaces was used based on [1], [2], [4]–[7]. To form an equidistant grid, the most lateral intercostal electrodes were positioned at a distance d from the MCL, which was equal to the distance between the PSL and MCL. In the 2nd intercostal space, one additional electrode was located between the PSL and the lateral margin of the sternum similar to [15] and [16]. Finally, electrodes for a 12-lead electrocardiogram (ECG) and pairs of electrodes over the left and right sternocleidomastoid muscle were also integrated. A common (ground) electrode was placed above the sternum as a bony part of the torso.

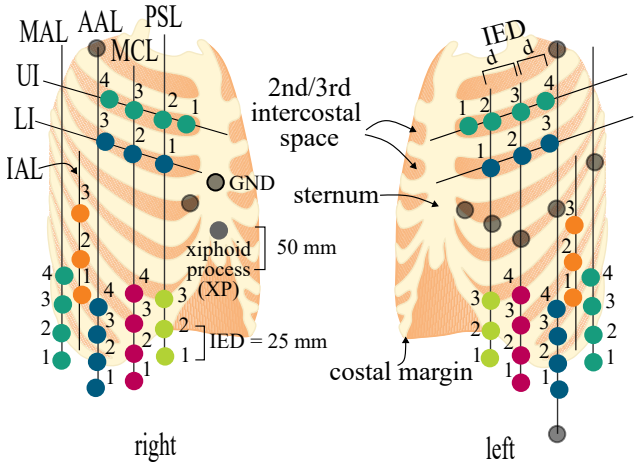

Fig. 1. The electrode scheme for quantitative comparison of differential leads based on anatomical lines (midaxillary line (MAL), anterior axillary line (AAL), midclavicular line (MCL), and parasternal line (PSL)) and bony landmarks. The inter axillary line (IAL) corresponds to the middle between the MAL and AAL. The ground electrode (GND) was placed on the sternum. The upper intercostal line (UI) is in the 2nd intercostal space and the lower intercostal line (LI) in the 3rd intercostal space. Inter electrode distances (IED) are marked. Gray unlabeled circles correspond to 12-lead electrocardiogram electrodes.

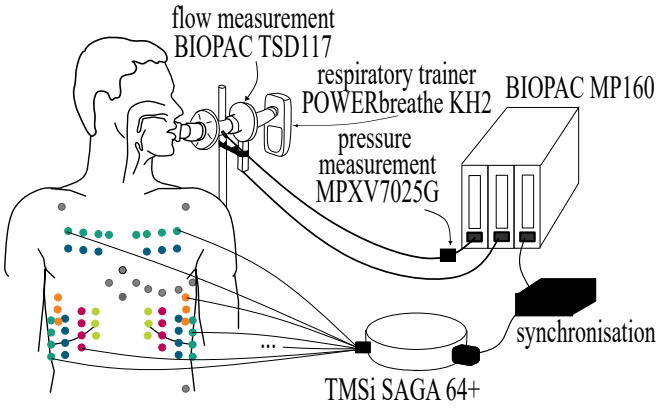

Fig. 2. Overview of the measurement setup: sEMG signals were recorded using the TMSi SAGA 64+ amplifier. The flow and pressure sensors were connected to the BIOPAC MP160 analysis device. For synchronization of sEMG and pneumatic signals, a microcontroller, sending a randomized square-wave signal to both recording devices, was added.

2) Signal Acquisition: Surface EMG, airway flow, and airway pressure data were acquired with the measurement setup depicted in Fig. 2. All 64 unipolar sEMG channels were recorded using the TMSi SAGA 64+ (TMSi, Oldenzaal, Netherlands) amplifier in average reference mode, which measures all signals against the average of all attached input channels. All sEMG signals were sampled at 2000 Hz. Prior to each measurement, electrode impedance values were checked and documented. Airway flow was measured using the TSD117B sensor and digitized using the DA100C differential bridge amplifier with the MP160 analysis device (all from BIOPAC Systems, Inc., Goleta, USA). The amplifier was set to a gain of 1000 and an analog low-pass filter with cutoff frequencies at 10 Hz was applied. Airway pressure was measured with the MPXV7025 sensor (NXP Semiconductors, Eindhoven, Netherlands) connected to the HLT100C transducer interface module (BIOPAC Systems, Inc., Goleta, USA) of the MP160 system. Both flow and pressure data were sampled at 2000 Hz.

To synchronize the sEMG signals with the pneumatic data, a microcontroller (JOY-IT MEGA2560R3, SIMAC Electronics GmbH, Neukirchen-Vluyn, Germany) generated a square wave signal with a randomized duty cycle and frequency. By recording this digital signal on both analysis devices (TMSi SAGA 64+ and MP160) the global time-shift could be corrected for during post-processing.

C. Study Protocol

Throughout the electrode application and protocol, subjects were in supine resting position with the torso elevated at 15 degree upright and their arms at their sides. The study procedure started with skin preparation, including cleaning with alcohol, slightly abrading, and applying a small amount of additional electrode gel to the pre-gelled electrodes. The electrode placement was carried out by two experienced investigators who carefully palpated the anatomical landmarks and verified the electrode positions according to the four-eyes principle. The study protocol was comprised of three different breathing maneuvers (quiet breathing (1), maximum inspiratory pressure (MIP) trials (2), and resistance breathing (3)), which were performed consecutively. Between maneuvers, breaks of 120 s were kept to avoid muscle fatigue. During signal acquisition, nasal air leaks were prevented by a nose clip. To get a measure of tonic muscle activity and random noise, a 60 s baseline measurement of muscle relaxation was recorded before all of the three respiratory maneuvers. To this end, subjects were asked to relax and perform quiet, shallow breathing without using the mouthpiece or the nose clip.

The first part of the protocol encompassed 300 s of quiet tidal breathing through the mouthpiece of the measurement setup without any additional load. Subjects were free to choose their own respiration pattern, i.e., no specifications were given regarding tidal volume and respiratory rate.

In the second step of the protocol, five maximum inspiratory pressure (MIP) maneuvers were performed to assess the global respiratory muscle strength. Subjects were instructed to exhale to the residual volume and subsequently inhale as forcefully as possible against a nearly occluded airway [22]. The MIP maneuver was carried out with the specific MIP program of the POWERbreathe KH2 (POWERbreathe International Ltd., Southam, UK), which was attached to the distal end of the setup. Breaks of 20 s were kept and verbal encouragement was given to reach maximum values. The highest pressure achieved was used as a reference value for resistance breathing.

The final step of the protocol, resistance breathing, was carried out with an inspiratory resistance level of 20 % of the MIP. The inspiratory load was set via the attached POWERbreath KH2. Subjects were instructed to perform 15 deep and forceful inspirations against the resistance with a freely chosen respiration pattern.

D. Signal Processing

Airway pressure and flow signals were smoothed using a $100\,\mathrm{ms}$ running mean filter. The tidal volume was calculated by breath-wise integration of the flow. Surface EMG and pneumatic data were synchronized by maximizing cross-correlation between the square wave signals recorded on both devices. The Pan-Tomkins algorithm was applied to Einthoven's lead II to detect the position of R-peaks within the sEMG data. Power line interference was removed from all sEMG channels using Butterworth stop-band filtering. Cardiac interference was then suppressed using a modified wavelet denoising algorithm similar to [23]. To this end, wavelet coefficients were calculated for all sEMG signals using the Daubechies tap-4 wavelet and 5 decomposition levels. Then, level-dependent adaptive thresholds were applied, which were calculated as multiples of the standard deviation using the robust noise estimator proposed in [23]. To increase sensitivity to the ECG artifact, lower wavelet thresholds were used in the region of the R-peak and the P-wave. Finally, after wavelet denoising, a $20\,\mathrm{Hz}$ Butterworth high-pass filter was applied to remove any remaining low-frequency interference. Envelopes for unipolar or differential leads were calculated via a $250\,\mathrm{ms}$ mean absolute value filter.

1) Outlier Detection: Due to the high number of EMG channels per subject, automated detection and removal of erroneous signals is essential. Electrode impedances were checked before each measurement in order to detect whether electrodes were completely detached — then, during post-processing, the goal was to exclude any remaining recordings with high baseline noise or artifacts separately in each maneuver. As a first step, the level of baseline noise was determined during the corresponding baseline measurements in each subject and unipolar channel. The noise amplitude was calculated using the first quartile of envelope values over a $30\,\mathrm{s}$ window. Then, we excluded channels if the baseline noise amplitude was higher than the Q_{95} quantile of baseline noise amplitudes of across channels. The latter was therefore calculated independently for each baseline measurement of the maneuver across all unipolar channels of the subject.

To detect other relevant sources of interference, such as motion or cable artifacts, the distribution of EMG waveforms across breaths was also analyzed. Accordingly a segmentation into inspiratory and expiratory phases was implemented by using zero-crossings in the flow signal. For both quiet and resistance breathing, breaths were normalized in length and an ensemble of EMG envelopes was formed across all breaths in each evaluated (bipolar) channel. Outliers were detected as samples that were more than three standard deviations from the ensemble mean, and the corresponding breaths were excluded from further analyses.

E. Data Analysis

The herein conducted analysis provides a quantitative comparison of diaphragm and intercostal sEMG channels.We used the following three metrics to quantify the signal-to-noise ratio of each channel, which are comparable to the ratios calculated in [8]. Firstly, the amplitudes reached during inspirations were related to the level of baseline noise during the baseline measurements. This was realized by forming the ratio

$$\mathrm{SNR}_{\mathrm{base}}\ (\mathrm{dB}) = 20 \cdot \log_{10} \frac{Q_{75}(\mathrm{sEMG}_{\mathrm{env,insp}})}{Q_{25}(\mathrm{sEMG}_{\mathrm{env,baseline}})}, \quad (1)$$

where $Q_{75}(\mathrm{sEMG}_{\mathrm{env,insp}})$ denotes the third quartile of inspiratory envelope values and $Q_{25}(\mathrm{sEMG}_{\mathrm{env,baseline}})$ is the first quartile of envelope values in the baseline measurement [1]. A high value indicates a good transmission of respiratory activity at a low level of noise due to tonic muscle activity or other external sources of interference, which is essential to detect changes in respiratory effort. Breaths whose baseline measurement was 1.5 times higher than the minimum breath envelope value were excluded. Secondly, the amount of crosstalk between inspiratory and expiratory muscles was approximated via

$$\mathrm{SNR}_{\mathrm{exp}}\ (\mathrm{dB}) = 20 \cdot \log_{10} \frac{Q_{75}(\mathrm{sEMG}_{\mathrm{env,insp}})}{Q_{75}(\mathrm{sEMG}_{\mathrm{env,exp}})}, \quad (2)$$

where the inspiratory EMG amplitude is defined as in equation (1) and is related to the expiratory EMG amplitude $Q_{75}(\mathrm{sEMG}_{\mathrm{env,exp}})$. A high value of this metric indicates that the inspiratory EMG is clearly distinguishable from other muscles that are active during expiration. A characteristic that is important in assessing the correct onset and offset times for evaluating ventilator-patient interactions. Note, if expiratory crosstalk is present $\mathrm{SNR}_{\mathrm{exp}}$ is lower than $\mathrm{SNR}_{\mathrm{base}}$. Thirdly, to quantify the impact of ECG interference, we employed a metric previously proposed by [23] defined as

$$\mathrm{SNR}_{\mathrm{EMG-ECG}}\ (\mathrm{dB}) = 10 \cdot \log_{10} \frac{\mathrm{P}(\mathrm{sEMG}_{\mathrm{raw}}(\neg\mathrm{insp} \wedge \mathrm{beat}))}{\mathrm{P}(\mathrm{sEMG}_{\mathrm{raw}}(\mathrm{insp} \wedge \neg\mathrm{beat}))}, \quad (3)$$

which was calculated on the raw (baseline-free) signal before ECG removal (denoted as $\mathrm{sEMG}_{\mathrm{raw}}$), refer to Fig. 3 for an illustrative excerpt of this signal. The metric relates the power of R-peaks during expirations, denoted by $\mathrm{sEMG}_{\mathrm{raw}}(\neg\mathrm{insp} \wedge \mathrm{beat})$, to the power of the inspiratory EMG in between R-peaks, denoted by $\mathrm{sEMG}_{\mathrm{raw}}(\mathrm{insp} \wedge \neg\mathrm{beat})$. Somewhat counterintuitively, many commonly used ECG removal algorithms, such as gating and wavelet denoising, benefit from large ECG artifacts. Therefore, to obtain a clean EMG signal, this metric should be high.

We focused on two groups of leads, which measure primarily diaphragm activity and intercostal activity, respectively. In both groups, we evaluated bilateral leads with electrodes positioned symmetrically on both sides of the rib cage and unilateral leads with electrodes only on one side. Additionally, for the diaphragm, we considered leads between the xiphoid process electrode and one electrode on the costal margin.

1) Statistics: The similarity between unipolar EMG signals was assessed via Pearson's correlation coefficient r, which was calculated on the raw EMG signal after removal of cardiac artifacts. For statistical analysis of the performance metrics, two commonly used electrode leads were selected as references for the diaphragm and intercostal muscles, respectively. In the case of the diaphragm, the bilateral lead with electrodes on the midclavicular line at the costal margin was used as a reference.

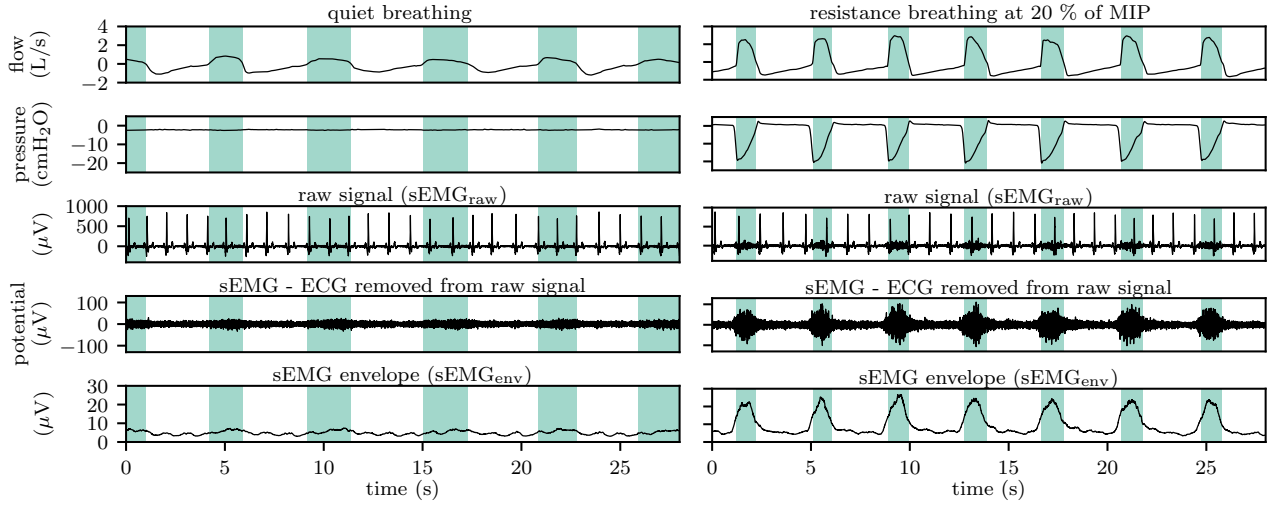

Fig. 3. Signal processing pipeline for representative samples of tidal quiet breathing and resistance breathing with inspiration phases marked in green. In the baseline-free raw signal, the electrical signal of the heart (electrocardiogram) is clearly visible. This prominent contaminant is removed and the sEMG envelope is calculated via a $250\,\mathrm{ms}$ mean absolute value filter.

For intercostal muscles, the bilateral lead with electrodes positioned on the parasternal line in the 2nd intercostal space was selected as a reference. To compare electrode leads within both groups against references, pairwise *t*-tests were performed for $\mathrm{SNR}_{\mathrm{base}}$, $\mathrm{SNR}_{\mathrm{exp}}$ and $\mathrm{SNR}_{\mathrm{EMG-ECG}}$. A *p*-value of less than 0.05 was considered significant. To account for multiple testings within sub-groups and to balance between type I and type II errors, the Bonferroni-Holm correction was used by adjusting the p-value between $0.05/T$ and 0.05 with T being the number of tests [24]. All results are reported as mean $\pm$ standard deviation.

TABLE II
CHARACTERISTIC OF FEMALE AND MALE SUBJECTS

Characteristic	Female ($n = 10$)	Male ($n = 10$)
age (years)	26.8 ± 3.43	26.6 ± 3.23
BMI ($\mathrm{kg/m^2}$)	23.99 ± 3.04	24.02 ± 2.77
MIP ($\mathrm{cmH_2O}$)	68.3 ± 20.1	103.9 ± 19.0
respiration rate (breaths/min)		
quiet breathing	13.02 ± 4.36	11.55 ± 2.59
resistance breathing	14.95 ± 7.81	15.67 ± 4.58
tidal volume (L)		
quiet breathing	0.64 ± 0.1	0.84 ± 0.2
resistance breathing	1.56 ± 0.55	1.95 ± 0.82

BMI: body-mass-index; MIP: maximum inspiratory pressure

III. RESULTS

The study included 10 female and 10 male young subjects with an age of 26.80 ± 3.43 years and 26.60 ± 3.23 years, respectively. The BMI was $23.99 \pm 3.04\,\mathrm{kg/m^2}$ for female and $24.02 \pm 2.77\ \mathrm{kg/m^2}$ for male participants. Table II reports meta-data and respiratory characteristics. Compared to age and BMI, which are quite consistent between male and female subjects, MIP showed a more pronounced difference with $68.3 \pm 20.1\,\mathrm{cmH_2O}$ and $103.9 \pm 19.0\,\mathrm{cmH_2O}$, respectively. These values are slightly lower than reported reference values [25]. However, it is documented that MIP values depend on body posture [26], i.e. lower values are observed in supine positions, and are also influenced by the measurement setup [22]. Respiratory rate was within the normal range for adults and slightly increased for resistance breathing [27]. For male participants, the tidal volume per breath of quiet breathing was 0.84 ± 0.2 L, which is slightly above the normal range of below $0.5\,\mathrm{L}$ expected for adults [27]. During resistance breathing, a substantial increase in tidal volume was noticeable for both male and female subjects.

The distribution of impedances prior to quiet breathing and resistance breathing for all 64 electrodes per subject are depicted in Fig. 4. The median impedance values ranged from $43.5\,\mathrm{k\Omega}$ to $183.5\,\mathrm{k\Omega}$ for quiet breathing. Despite extensive skin preparation, a few electrodes reached higher values of up to $380\,\mathrm{k\Omega}$. The median impedance value decreased with measurement time. Thus, for resistance breathing, the median impedance values ranged from $38\,\mathrm{k\Omega}$ to $173\,\mathrm{k\Omega}$. The range of values is higher than what is recommended in the literature [28], but greater abrasion of the skin was not considered feasible due to the large area of skin involved in the measurement.

An imbalance between impedance values mainly affects the amplification of common mode signals, e.g., physiological crosstalk or external noise. Thus, to reduce noise, the general recommendation is that impedances should be low and within a narrow range [29]. To better assess this effect in our data, we analyzed the relation between impedance values and the baseline noise ($Q_{25}(\mathrm{sEMG_{env,baseline}})$). For both phases of the study, we found no correlation between noise and impedances, as shown in Fig. 5. Thus, we concluded that skin-electrode impedance was not a significant confounder for the evaluation.

The detection of outliers with respect to the baseline noise amplitude led to the exclusion of 60 channels in both quiet breathing and resistance breathing phases across all subjects, which is also plotted in Fig. 5. On average 75 breaths per lead were detected as outliers and excluded from the analysis of quiet breathing based on the envelope ensembles, resulting in an average of 472 breaths per lead evaluated across all subjects. For resistance breathing, on average 58 breaths per

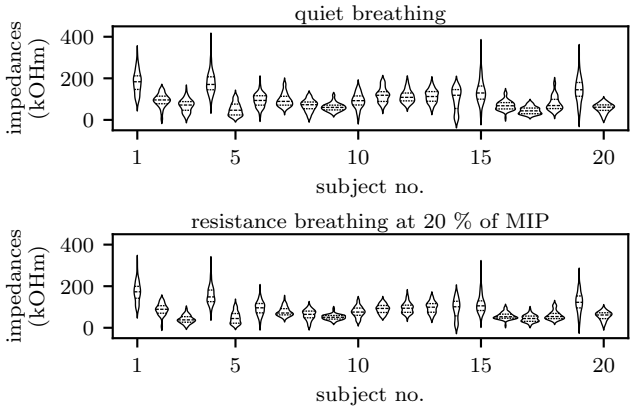

Fig. 4. Impedance values documented prior to quiet breathing (top) and resistance breathing (bottom) for all 64 unipolar electrodes per subject

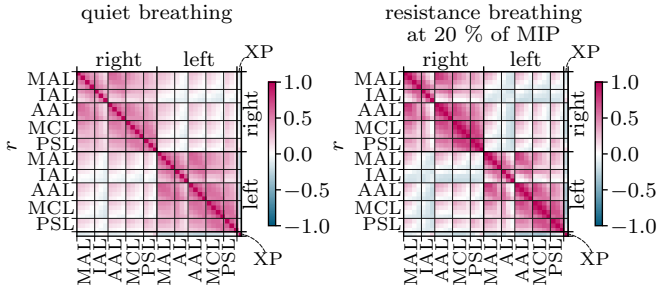

Fig. 6. Pearson correlation coefficients averaged over all subjects for unipolar leads that measure the diaphragmatic activity at quiet breathing (left) and resistance breathing (right). MAL: midaxillary line; IAL: inter axillary line; AAL: anterior axillary line; MCL: midclavicular line; PSL: parasternal line; XP: xiphoid process electrode.

lead were detected as outliers and 254 breaths per lead were included in the analysis across all subjects. The reasons for outliers were both of technical, e.g. cable or electrode movements, and had a physiological origin, e.g. crosstalk from limb muscles.

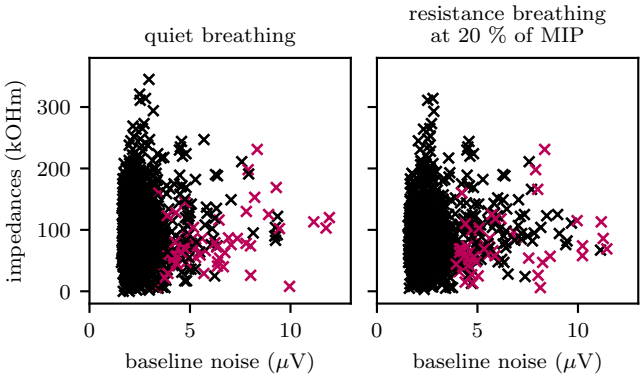

Fig. 5. Baseline noise calculated as the first quartile of the unipolar baseline measurement envelopes and corresponding impedance values for quiet breathing (left) and resistance breathing (right). Each data point corresponds to one subject and unipolar channel. Detected outliers higher than the $\boldsymbol{Q_{95}}$ quantile of all baseline noise values of the subject are marked in red.

A. Diaphragm

Fig. 6 shows correlation coefficients r of all unipolar leads measuring diaphragm activity averaged over all subjects. During quiet tidal breathing, positive correlation was found for electrodes located closely together on one side of the rib cage. One exception is configurations with electrodes in the 6th and 7th intercostal spaces on the IAL, where only weak positive correlation is visible. Similarly, weak or no correlation was present for electrodes placed on opposite sides of the rib cage. For resistance breathing at 20 % of MIP a very similar pattern was observed, although here positive correlation increased even more strongly towards the diagonal for both unilateral matrix sub-blocks.

The performance metrics results are depicted in Fig. 7. Matrices of average performance metrics for all electrode pairs are provided in panel A and C. Here, maxima of $\mathrm{SNR_{base}}$ and $\mathrm{SNR_{exp}}$ are mainly discernible along the MCL and IAL as well as their intersections. $\mathrm{SNR_{EMG-ECG}}$ generally appears to be higher in bilateral leads than in unilateral leads and is highest for any leads involving the xiphoid process electrode XP.

The distribution of performance metrics for a subset of leads is depicted in panels B and D. The reference channel (with electrodes positioned bilaterally at MCL2) attained an $\mathrm{SNR_{base}}$ of $5.36 \pm 2.82\,\mathrm{dB}$ and $15.56 \pm 3.94\,\mathrm{dB}$ as well as an $\mathrm{SNR_{exp}}$ of 2.55 ± 1.72 dB and $7.57 \pm 3.35\,\mathrm{dB}$ during quiet breathing and resistance breathing, respectively. The only symmetric, bilateral lead with significantly higher $\mathrm{SNR_{base}}$ values was the position $2.5\,\mathrm{cm}$ above the costal margin (MCL3), reaching an $\mathrm{SNR_{base}}$ of $6.00 \pm 3.04\,\mathrm{dB}$ and $17.42 \pm 4.71\,\mathrm{dB}$ for quiet breathing and resistance breathing, respectively. This lead also attained a significantly higher $\mathrm{SNR_{exp}}$ value of 9.05 ± 2.71 dB during resistance breathing. Compared to the reference channel, most bilateral leads on the MAL and AAL had significantly lower $\mathrm{SNR_{base}}$ and $\mathrm{SNR_{exp}}$ values. For the MAL and AAL the highest average $\mathrm{SNR_{base}}$ and $\mathrm{SNR_{exp}}$ was reached at a higher position, 5cm above the costal margin. Across all symmetric, bilateral leads the largest ECG artifact was found $5\,\mathrm{cm}$ above the costal margin (MCL4) with an $\mathrm{SNR_{EMG-ECG}}$ of $27.03 \pm 2.95\,\mathrm{dB}$ during quiet breathing.

Compared to the reference channel, most of the unilateral leads shown in panel B and D of Fig. 7 also had a significantly lower $\mathrm{SNR_{base}}$ and $\mathrm{SNR_{exp}}$. Notably, the commonly used unilateral positions in the 7th and 8th intercostal space (denoted IAL1-IAL2) attained lower average values for $\mathrm{SNR_{base}}$ and $\mathrm{SNR_{exp}}$, but this difference was only significant for the right body side. An interesting finding was that a previously unknown unilateral combination of electrodes between the MCL and the IAL achieved comparable values on average than the bilateral reference. Compared to the bilateral reference channel, ECG interference was significantly lower for most of the considered unilateral leads.

Finally, the leads with one electrode above the xiphoid process and the other electrode on the MCL or PSL at the costal margin had similar range of values for $\mathrm{SNR_{base}}$ and $\mathrm{SNR_{exp}}$ as the bilateral reference. The $\mathrm{SNR_{EMG-ECG}}$ was

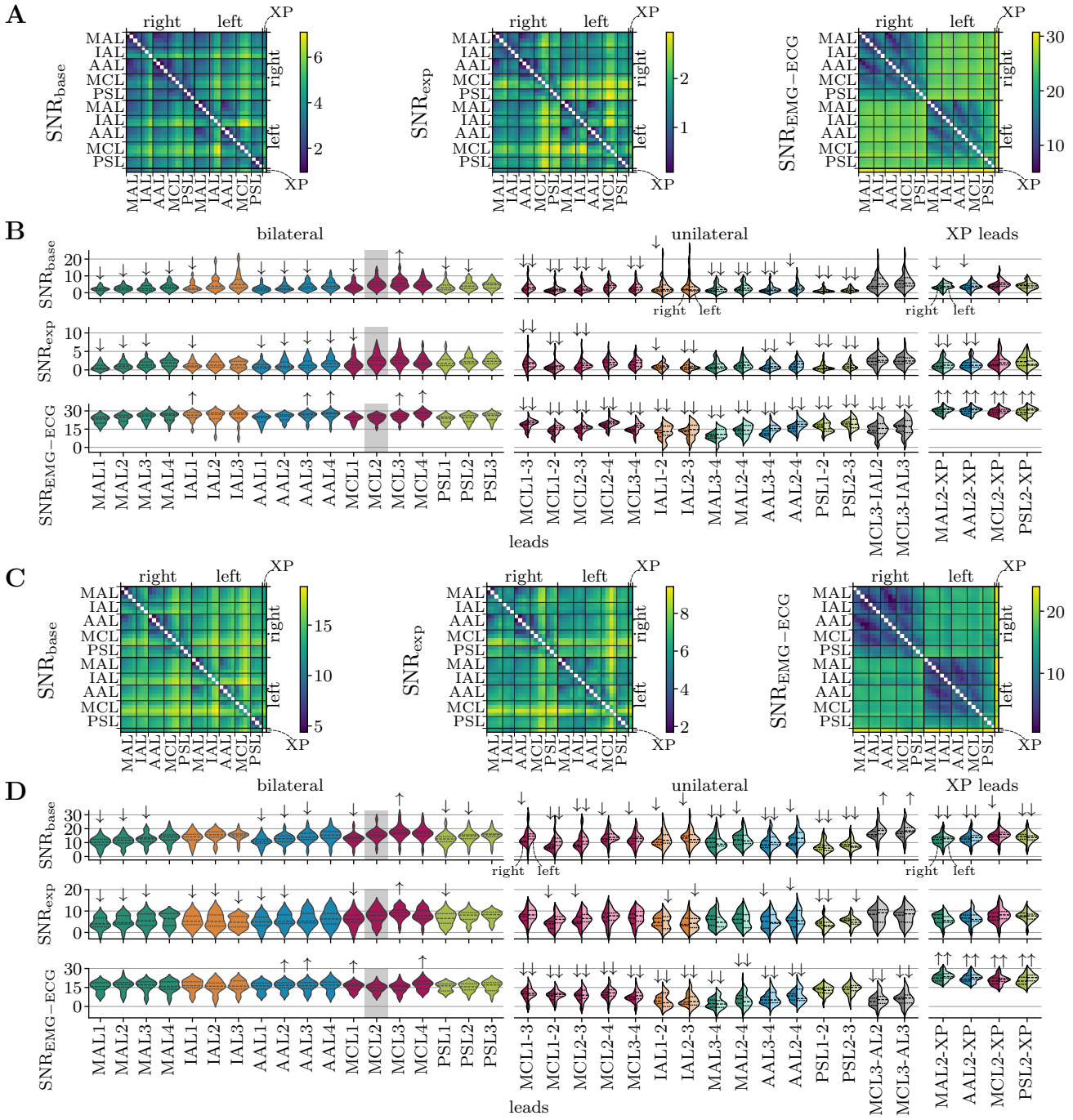

Fig. 7. Quantitative evaluation of differential electrode leads that measure predominantly diaphragmatic activity: Matrices with performance metrics averaged over all subjects for quiet breathing and resistance breathing are shown in panel A and C, respectively. The distribution of performance metrics for a selected subset of bilateral and unilateral leads for quiet breathing and resistance breathing is shown in panel B and D as violin plots, respectively. Statistically significant differences ($p < 0.05$) compared to the reference lead (gray shaded) are marked by ↑ for positive deviations and by ↓ for negative deviations. - MAL: midaxillary line; IAL: inter axillary line; AAL: anterior axillary line; MCL: midclavicular line; PSL: parasternal line; XP: xiphoid process electrode.

highest for these leads, on average reaching almost 30 dB during quiet breathing.

B. Intercostal Muscles

Fig. 8 shows average correlation coefficients r of unipolar leads recording intercostal muscle activity, which includes all electrodes in the 2nd and 3rd intercostal space (denoted UI and LI). In this case as well, electrodes on one side of the chest showed positive correlation, while electrodes on opposite sides of the torso correlated only weakly or not at all. Similarly to diaphragmatic leads, correlation coefficients during resistance breathing were higher than during quiet breathing.

Results of performance metrics for the intercostal muscles are shown in Fig. 9. Panels A and B provide matrices of performance metrics for all electrode pairs. Overall, it is

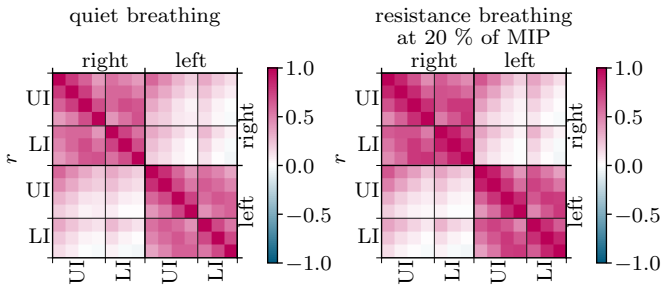

Fig. 8. Pearson correlation coefficients averaged over all subjects for unipolar leads that measure the intercostal muscle activity at quiet breathing (left) and resistance breathing (right). UI: upper intercostal line (2nd intercostal space); LI: lower intercostal line (3rd intercostal space).

more difficult to identify clear trends here. One thing that can be recognised is that electrodes that are close to each other, i.e., directly along the matrix diagonal, have low values for $\mathrm{SNR}_{\mathrm{base}}$ and $\mathrm{SNR}_{\mathrm{exp}}$. It can also be clearly seen that $\mathrm{SNR}_{\mathrm{EMG-ECG}}$ increases towards the left side of the body.

Panels C and D depict distributions of performance metrics for an interesting subset of leads. The reference lead with electrodes positioned bilaterally on the PSL in the 2nd intercostal space (UI2) had an $\mathrm{SNR}_{\mathrm{base}}$ of $5.62 \pm 2.47\,\mathrm{dB}$ and $13.52 \pm 3.15\,\mathrm{dB}$ as well as an $\mathrm{SNR}_{\mathrm{exp}}$ of $2.59 \pm 1.82\,\mathrm{dB}$ and $6.26 \pm 2.21\,\mathrm{dB}$ during quiet breathing and resistance breathing, respectively. None of the other symmetric, bilateral leads had higher average values for $\mathrm{SNR}_{\mathrm{exp}}$. Though, one symmetric, bilateral leads with more lateral electrodes in the 2nd intercostal space (UI4) attained slightly higher average values for $\mathrm{SNR}_{\mathrm{base}}$, which however was not significant. Notably, the position between the PSL and the sternum, which has been used in several studies, on average performed worse than the reference regarding both $\mathrm{SNR}_{\mathrm{base}}$ and $\mathrm{SNR}_{\mathrm{exp}}$. None of the unilateral, intercostal leads shown in panels C and D reached higher average performance values than the bilateral reference for $\mathrm{SNR}_{\mathrm{base}}$ and $\mathrm{SNR}_{\mathrm{exp}}$. All of the tested unilateral leads on the left side of the thorax showed a significantly stronger ECG interference.

IV. Discussion

In this study, we recorded the spatial distribution of electrical potentials generated on the skin surface during breathing to provide the most comprehensive evaluation of respiratory sEMG electrode positions to date. We performed a quantitative comparison based on different performance metrics ($\mathrm{SNR}_{\mathrm{base}}$, $\mathrm{SNR}_{\mathrm{exp}}$, and $\mathrm{SNR}_{\mathrm{EMG-ECG}}$), which allow us to make recommendations for the placement of electrodes.

In this work, we focused on *inspiratory* muscles and cases where the overall respiratory activity is low, e.g., critically ill patients in the intensive care unit. In these settings, a high inspiratory sEMG amplitude and minimal expiratory crosstalk is necessary to quantify patient-ventilator interactions by detecting inspiratory onset and offset times. For clinical applicability, we therefore aim to maximize $\mathrm{SNR}_{\mathrm{base}}$ and $\mathrm{SNR}_{\mathrm{exp}}$. Note that for these applications, a difference of a few decibels can have a substantial impact on the interpretability of signals. Since researchers have relied on signal processing techniques like gating or wavelet denoising to remove the ECG artifact [1], [7], [30], which benefit from large R-peaks, $\mathrm{SNR}_{\mathrm{EMG-ECG}}$ should also be maximized.

For measuring diaphragm activity, our results support the use of bilateral positions on the MCL, as previously used in many studies [1], [2], [4]–[7]. Notably, for the bilateral setup, none of the more lateral or medial body lines (MAL, AAL, and PSL) attained higher $\mathrm{SNR}_{\mathrm{base}}$ and $\mathrm{SNR}_{\mathrm{exp}}$ values. We also found that the highest activity for bilateral leads was not directly on the costal margin, but in the zone of apposition, $2.5\,\mathrm{cm}$ superior to the costal margin on the MCL and at least $5\,\mathrm{cm}$ superior to the costal margin on the MAL and AAL. Our results are in agreement with Lansing and Savelle [19], who reported that peak activity with unilateral leads was superior to the costal margin. We assume that favourable measurement conditions are reached when the bilateral electrodes are in the zone of apposition and above the costal cartilage, which is a tissue with higher electric conductivity compared to the bony parts of the ribs [31].

Our study also provides the first comparison between bilateral and unilateral diaphragm leads. We found that unilateral leads did not significantly outperform the bilateral configuration. In particular, most unilateral leads with small inter electrode distance shown in panels B and D of Fig. 7 had significantly smaller $\mathrm{SNR}_{\mathrm{base}}$ and $\mathrm{SNR}_{\mathrm{exp}}$ values, which can be attributed to the higher correlation between the corresponding unipolar signals visible in Fig. 6, which in turn causes a reduction of signal power in the differential signal. Compared to bilateral leads, most unilateral leads had small ECG artifacts indicated by $\mathrm{SNR}_{\mathrm{EMG-ECG}}$, thus, complicating detection and separation of R-peaks. The best performing unilateral leads were those with large inter electrode distance, e.g., a combination of one electrode on the MCL and another electrode in the 6th to 8th intercostal space (IAL1–3) or on the sternum superior to the xiphoid process. In contrast, one of the most utilized unilateral electrode setups between the 7th and 8th intercostal space on the IAL [8]–[11] achieved relatively low values. In particular, these leads were more influenced by expiratory crosstalk, which led to significantly lower $\mathrm{SNR}_{\mathrm{exp}}$. One reason for this could be that the IAL electrodes are positioned at a higher transverse level and record a mixture of intercostal and diaphragmatic muscle activity.

From our results, we make the following conclusions. Bilateral leads are in general best suited for measuring small sEMG signals when the respiratory effort is low and ECG artifacts can be removed using gating or wavelet denoising. However, there are clinically relevant situations, e.g., unilateral diaphragmatic paresis or highly active patients with chronic obstructive pulmonary disease, where unilateral recordings may be more appropriate. In general, depending on the clinical application, electrode setups with smaller pickup volumes and EMG amplitudes may be preferable if this helps to reduce the influence of crosstalk.

For intercostal muscles, dependence on electrode positions was less prominent. The bilateral, parasternal position in the 2nd intercostal space is a good first choice, but other leads were in a similar value range concerning the considered performance metrics. In particular, there seems to be some flexibility

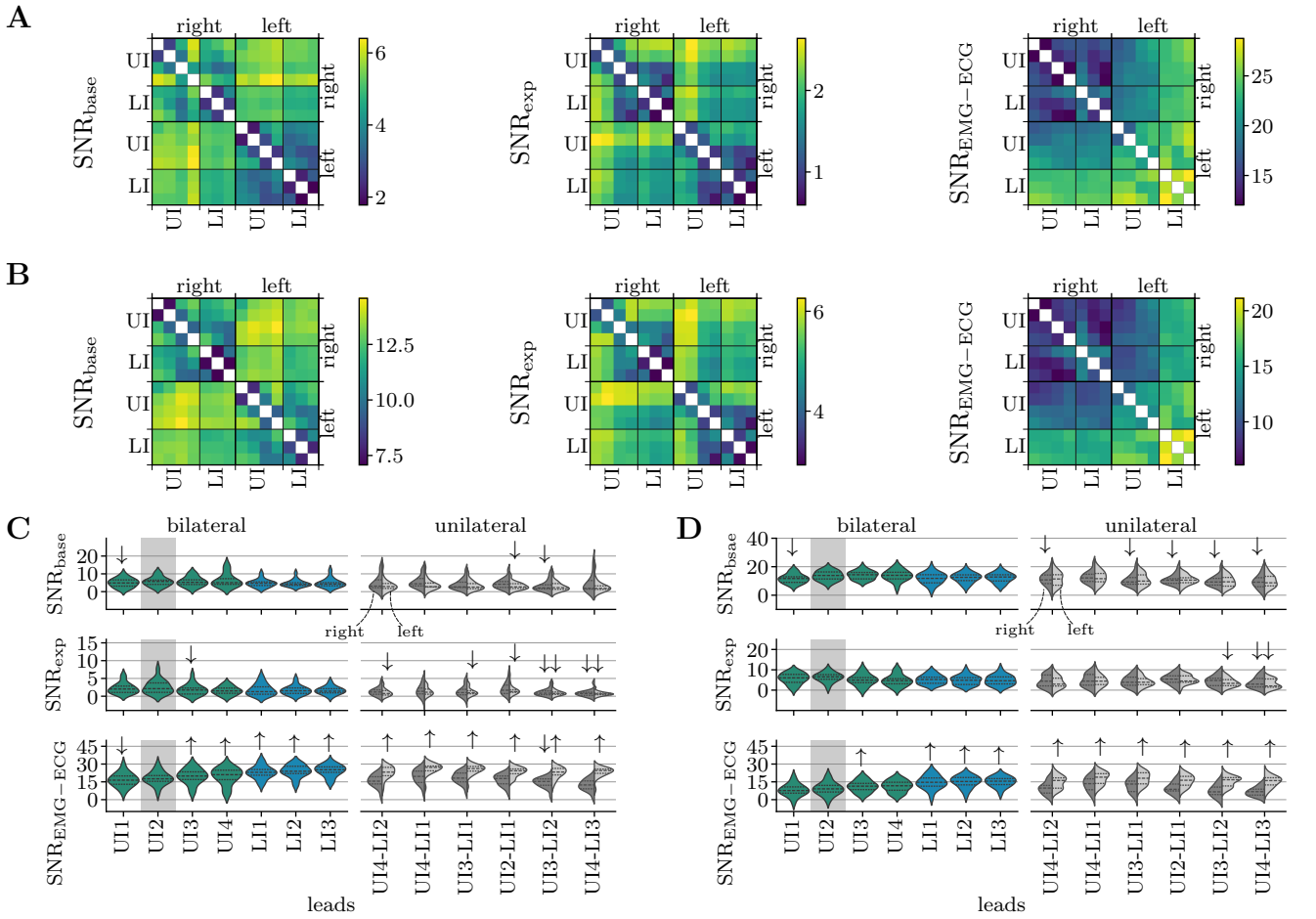

Fig. 9. Quantitative evaluation of differential electrode leads that measure intercostal muscle activity: Matrices with performance metrics averaged over all subjects for quiet breathing and resistance breathing are shown in panel A and B, respectively. The distribution of performance metrics for a selected subset of bilateral and unilateral leads for quiet breathing and resistance breathing is shown in panel C and D as violin plots, respectively. Statistically significant differences ($p < 0.05$) compared to the reference lead (gray shaded) are marked by ↑ for positive deviations and by ↓ for negative deviations. - UI: upper intercostal line (2nd intercostal space); LI: lower intercostal line (3rd intercostal space).

of positioning electrodes more lateral, e.g., when parts of the thorax are covered by bandages or wounds due to surgery, or more medial when muscle crosstalk due to arm/shoulder movements is a concern. As for the diaphragm, unilateral leads do not appear to outperform the bilateral configuration. The amount of ECG interference can be influenced via the electrode position as $SNR_{EMG-ECG}$ was larger on the left side of the body.

Our study has revealed considerable differences in the performance of bipolar electrode leads for both diaphragmatic and intercostal muscle activity recording. These differences are even evident between commonly used electrode leads. The findings highlight once more that standardization of respiratory sEMG measurements is important and may not only improve comparability between studies, but also increase clinical acceptance of this non-invasive monitoring tool. With this study, we contribute to closing this research gap. In contrast to the earlier work by Lansing et al. [19], our setup enables the simultaneous comparison of unilateral and bilateral electrode leads for the diaphragm and the intercostal muscles.

Several limitations need to be acknowledged. Firstly, a young and healthy subject population was enrolled. However, critically ill patients show substantial changes in respiratory muscle function, suffering from muscle weakness, pathological breathing patterns, and altered diaphragm shape and position, e.g., due to positive end-expiratory pressure PEEP, which is common in ventilated patients [32]–[35]. Depending on the applied PEEP value a substantial caudal displacement of the diaphragm and a shortening of the zone of apposition is observable [35]. In these cases, the selection of the optimal electrode lead may shift in a caudal direction, an effect that was also observed by Lansing and Savelle [19] at high lung volumes. Secondly, study subjects were characterized to have a relatively low BMI range. This is also in contrast to the intensive care population, where overweight or obesity is common [36], [37]. It is well known that a thicker layer of subcutaneous tissue affects the sEMG signal amplitudes [38], [39], potentially reducing SNRs or even causing the EMG to be undetectable. However, the impact on specific electrode leads may vary, as it depends on the specific body composition and subcutaneous tissue distribution. Whether our recommendations also apply to cohorts with a higher BMI range will be subject to further research.

V. Conclusion

We have conducted a comprehensive comparison of electrode leads for measuring respiratory muscle activity via skin surface electrodes. Our findings in 20 healthy and young adults confirm that bilateral electrode positions offer the best performance with respect to the inspiratory signal-to-noise ratio. We recommend to measure the diaphragm sEMG using a pair of electrodes on the midclavicular lines $2.5\,\mathrm{cm}$ above the costal margin. The intercostal EMG can be measured with a pair of electrodes on the parasternal line in the second intercostal space, but there is some flexibility of moving electrodes more lateral or medial. This analysis represents a first step towards standardization of respiratory sEMG measurements, which is essential for clinical acceptance of the method and in turn will foster clinical application.

References

[1] J. Graßhoff *et al.*, "Surface EMG-based quantification of inspiratory effort: a quantitative comparison with Pes," *Critical Care*, vol. 25, no. 1, p. 441, Dec. 2021.

[2] J. Sauer *et al.*, "Automated characterization of patient–ventilator interaction using surface electromyography," *Annals of Intensive Care*, vol. 14, no. 1, p. 32, Feb. 2024.

[3] A. H. Jonkman *et al.*, "Analysis and applications of respiratory surface emg: report of a round table meeting," *Critical Care*, vol. 28, no. 1, Jan. 2024.

[4] M. L. Duiverman *et al.*, "Respiratory muscle activity and patient-ventilator asynchrony during different settings of noninvasive ventilation in stable hypercapnic COPD: does high inspiratory pressure lead to respiratory muscle unloading?" *International Journal of Chronic Obstructive Pulmonary Disease*, vol. 12, pp. 243–257, Jan. 2017.

[5] G. Bellani *et al.*, "Measurement of Diaphragmatic Electrical Activity by Surface Electromyography in Intubated Subjects and Its Relationship With Inspiratory Effort," *Respiratory Care*, vol. 63, no. 11, pp. 1341–1349, Nov. 2018.

[6] M. L. Duiverman *et al.*, "Reproducibility and responsiveness of a noninvasive EMG technique of the respiratory muscles in COPD patients and in healthy subjects," *Journal of Applied Physiology*, vol. 96, no. 5, pp. 1723–1729, May 2003.

[7] M. Pozzi *et al.*, "Accessory and Expiratory Muscles Activation During Spontaneous Breathing Trial: A Physiological Study by Surface Electromyography," *Frontiers in Medicine*, vol. 9, p. 814219, Mar. 2022.

[8] L. Estrada-Petrocelli *et al.*, "Evaluation of Respiratory Muscle Activity by Means of Concentric Ring Electrodes," *IEEE Transactions on Biomedical Engineering*, vol. 68, no. 3, pp. 1005–1014, Mar. 2021.

[9] M. Lozano-Garcia *et al.*, "Noninvasive Assessment of Inspiratory Muscle Neuromechanical Coupling During Inspiratory Threshold Loading," *IEEE Access*, vol. 7, pp. 183 634–183 646, 2019.

[10] I. C. M. Ortega *et al.*, "Assessment of weaning indexes based on diaphragm activity in mechanically ventilated subjects after cardiovascular surgery. A pilot study," *Revista Brasileira de Terapia Intensiva*, vol. 29, no. 2, pp. 213–221, Apr.–Jun. 2017.

[11] M. Rafols-de Urquia *et al.*, "Evaluation of a Wearable Device to Determine Cardiorespiratory Parameters From Surface Diaphragm Electromyography," *IEEE Journal of Biomedical and Health Informatics*, vol. 23, no. 5, pp. 1964–1971, Sep. 2019.

[12] J. F. Alonso *et al.*, "Evaluation of respiratory muscles activity by means of cross mutual information function at different levels of ventilatory effort," *IEEE Transactions on Biomedical Engineering*, vol. 54, no. 9, pp. 1573–1582, Sep. 2007.

[13] G. Younis *et al.*, "Differences between diaphragmatic compound muscle action potentials recorded from over the sternum and lateral chest wall in healthy subjects," *Scientific Reports*, vol. 12, no. 1, p. 8925, May 2022.

[14] R. Chen *et al.*, "Phrenic nerve conduction study in normal subjects," *Muscle & Nerve*, vol. 18, no. 3, pp. 330–335, Mar. 1995.

[15] C. Bureau *et al.*, "Proportional assist ventilation relieves clinically significant dyspnea in critically ill ventilated patients," *Annals of Intensive Care*, vol. 11, no. 1, p. 177, Dec. 2021.

[16] M. Schmidt *et al.*, "Dyspnea and surface inspiratory electromyograms in mechanically ventilated patients," *Intensive Care Medicine*, vol. 39, no. 8, pp. 1368–1376, Aug. 2013.

[17] T. Ritz *et al.*, "Evaluation of a Respiratory Muscle Biofeedback Procedure-Effects on Heart Rate and Dyspnea," *Applied Psychophysiology and Biofeedback*, vol. 31, no. 3, pp. 253–261, Sep. 2006.

[18] R. W. van Leuteren *et al.*, "Diaphragmatic electromyography in preterm infants: The influence of electrode positioning," *Pediatric Pulmonology*, vol. 55, no. 2, pp. 354–359, Feb. 2020.

[19] R. Lansing and J. Savelle, "Chest surface recording of diaphragm potentials in man," *Electroencephalography and Clinical Neurophysiology*, vol. 72, no. 1, pp. 59–68, Jan. 1989.

[20] J. C. Glerant *et al.*, "Diaphragm electromyograms recorded from multiple surface electrodes following magnetic stimulation," *The European Respiratory Journal*, vol. 27, no. 2, pp. 334–342, Feb. 2006.

[21] A. Oltmann *et al.*, "Respiratory sEMG measurements for quantitative comparison of bipolar electrode leads," in *ISEK XXIV - 2024 ISEK Abstract Book*, International Society of Elektromyography and Kinesiologie, Ed., Jun. 2024.

[22] American Thoracic Society/European Respiratory Society, "Statement on respiratory muscle testing," *American Journal of Respiratory and Critical Care Medicine*, vol. 166, no. 4, pp. 518–624, Aug. 2002.

[23] E. Petersen *et al.*, "Removing Cardiac Artifacts From Single-Channel Respiratory Electromyograms," *IEEE Access*, vol. 8, pp. 30 905–30 917, 2020.

[24] R. A. Armstrong, "When to use the Bonferroni correction," *Ophthalmic & Physiological Optics : The Journal of the British College of Ophthalmic Opticians (Optometrists)*, vol. 34, no. 5, pp. 502–508, Sep. 2014.

[25] I. M. B. Sclauser Pessoa *et al.*, "Reference values for maximal inspiratory pressure: a systematic review," *Canadian Respiratory Journal*, vol. 21, no. 1, pp. 43–50, Jan.–Feb. 2014.

[26] R. Costa *et al.*, "Body position influences the maximum inspiratory and expiratory mouth pressures of young healthy subjects," *Physiotherapy*, vol. 101, no. 2, pp. 239–241, Jun. 2015.

[27] R. Brandes *et al.*, Eds., *Physiologie des Menschen: mit Pathophysiologie: mit 850 Farbabbildungen*. Berlin [Heidelberg]: Springer, 2019.

[28] G. Piervirgili *et al.*, "A new method to assess skin treatments for lowering the impedance and noise of individual gelled ag–agcl electrodes," *Physiological Measurement*, vol. 35, no. 10, p. 2101, Oct. 2014.

[29] R. Merletti and G. Cerone, "Tutorial. surface emg detection, conditioning and pre-processing: Best practices," *Journal of Electromyography and Kinesiology*, vol. 54, p. 102440, Oct. 2020.

[30] J. L. Lokin *et al.*, "Transesophageal Versus Surface Electromyography of the Diaphragm in Ventilated Subjects," *Respiratory Care*, vol. 65, no. 9, pp. 1309–1314, Sep. 2020.

[31] C. Baumgartner *et al.*, "IT'IS Database for Thermal and Electromagnetic Parameters of Biological Tissues, Version 4.2," 2024. [Online]. Available: https://itis.swiss/virtual-population/tissue-properties/overview/

[32] M. Dres *et al.*, "Critical illness-associated diaphragm weakness," *Intensive Care Medicine*, vol. 43, no. 10, pp. 1441–1452, Sep. 2017.

[33] J. Lindqvist *et al.*, "Positive End-Expiratory Pressure Ventilation Induces Longitudinal Atrophy in Diaphragm Fibers," *American Journal of Respiratory and Critical Care Medicine*, vol. 198, no. 4, pp. 472–485, Aug. 2018.

[34] R. Warnaar *et al.*, "Advanced waveform analysis of diaphragm surface emg allows for continuous non-invasive assessment of respiratory effort in critically ill patients at different peep levels," *Critical Care*, vol. 28, p. 195, Jun. 2024.

[35] D. Jansen *et al.*, "Positive end-expiratory pressure affects geometry and function of the human diaphragm," *Journal of Applied Physiology*, vol. 131, no. 4, pp. 1328–1339, Oct. 2021.

[36] A. de Jong *et al.*, "Medical Versus Surgical ICU Obese Patient Outcome: A Propensity-Matched Analysis to Resolve Clinical Trial Controversies," *Critical Care Medicine*, vol. 46, no. 4, pp. e294–e301, Apr. 2018.

[37] Y. Sakr *et al.*, "Being Overweight Is Associated With Greater Survival in ICU Patients: Results From the Intensive Care Over Nations Audit," *Critical Care Medicine*, vol. 43, no. 12, pp. 2623–2632, Dec. 2015.

[38] C. Nordander *et al.*, "Influence of the subcutaneous fat layer, as measured by ultrasound, skinfold calipers and BMI, on the EMG amplitude," *European Journal of Applied Physiology*, vol. 89, no. 6, pp. 514–519, Aug. 2003.

[39] D. Farina and A. Rainoldi, "Compensation of the effect of sub-cutaneous tissue layers on surface EMG: a simulation study," *Medical Engineering & Physics*, vol. 21, no. 6-7, pp. 487–497, Jul.–Sep. 1999.